GA–A22999

CONF-981064--

PROGRESS TOWARDS SUSTAINMENT OF ADVANCED TOKAMAK MODES IN DIII–D

by

B.W. RICE, K.H. BURRELL, J.R. FERRON, C.M. GREENFIELD, G.L. JACKSON, L.L. LAO, R.J. LA HAYE, T.C. LUCE, B.W. STALLARD, E.J. STRAIT, E.J. SYNAKOWSKI, T.S. TAYLOR, A.D. TURNBULL, and M.R. WADE

MASTER

DISTRIBUTION OF THIS DOCUMENT IS UNLIMITED

RECEIVED
JAN 11 1999
OSTI

DECEMBER 1998

GENERAL ATOMICS

DISCLAIMER

This report was prepared as an account of work sponsored by an agency of the United States Government. Neither the United States Government nor any agency thereof, nor any of their employees, make any warranty, express or implied, or assumes any legal liability or responsibility for the accuracy, completeness, or usefulness of any information, apparatus, product, or process disclosed, or represents that its use would not infringe privately owned rights. Reference herein to any specific commercial product, process, or service by trade name, trademark, manufacturer, or otherwise does not necessarily constitute or imply its endorsement, recommendation, or favoring by the United States Government or any agency thereof. The views and opinions of authors expressed herein do not necessarily state or reflect those of the United States Government or any agency thereof.

DISCLAIMER

Portions of this document may be illegible in electronic image products. Images are produced from the best available original document.

GA–A22999

PROGRESS TOWARDS SUSTAINMENT OF ADVANCED TOKAMAK MODES IN DIII–D

by

B.W. RICE,† K.H. BURRELL, J.R. FERRON, C.M. GREENFIELD, G.L. JACKSON, L.L. LAO, R.J. LA HAYE, T.C. LUCE, B.W. STALLARD,† E.J. STRAIT, E.J. SYNAKOWSKI,‡ T.S. TAYLOR, A.D. TURNBULL, and M.R. WADE◊

This is a preprint of a paper to be presented at the 17th International Atomic Energy Agency Fusion Energy Conference, October 19–24, 1998, Yokohama, Japan, and to be published in the *Special Issue of Nuclear Fusion.*

†Lawrence Livermore National Laboratory
‡Princeton Plasma Physics Laboratory
◊Oak Ridge National Laboratory

Work supported by
the U.S. Department of Energy
under Contracts DE-AC03-89ER51114, DE-AC02-76CH03073,
DE-AC05-96OR22464, and W-7405-ENG-48

GA PROJECT 3466
DECEMBER 1998

ABSTRACT

Improving confinement and beta limits simultaneously in long-pulse ELMy H–mode discharges is investigated. The product $\beta_N H_{98y}$ serves as a useful figure-of-merit for performance, where $\beta_N \equiv \beta/(I/aB)$ and H_{98y} is the ratio of the thermal confinement time relative to the most recent ELMy H–mode confinement scaling established by the ITER confinement database working group. In discharges with $q_0 \sim 1$ (no sawteeth) and discharges with $q_{min} > 1.5$ and negative central magnetic shear, $\beta_N \sim 2.9$ and $H_{98y} \sim 1.4$ are sustained forup to 2 s. Although peaked profiles are observed, steep internal transport barriers are not present. Further increases in β_N in these discharges is limited by neoclassical tearing modes (NTM) in the positive shear region. In another recently developed regime, $\beta_N \sim 3.8$ and $H_{98y} \sim 1.8$ has been sustained during large infrequent ELMs in non-sawtoothing discharges with $q_0 \sim 1$. This level of performance is similar to that obtained in ELM-free regimes such as VH–mode. The limitation on β_N and pulse length in these discharges is also the onset of NTMs.

1. INTRODUCTION

Advanced Tokamak (AT) operating modes have been successful in improving the fusion performance of many existing tokamaks, as evidenced by the record D-D fusion reactivity achieved in DIII–D [1], JT-60U [2], and JET [3]. Through optimization of the plasma shape and radial profiles, AT modes lead to improved confinement, higher β, and higher bootstrap fraction relative to standard ELMy H–mode. Improvements are observed in many different regimes such as VH–mode, negative central shear (NCS) with an internal transport barrier (ITB), supershots, high β_p, and high ℓ_i. To date, however, the duration of peak performance in all of these modes is limited to a few energy confinement times (τ_E), generally as a consequence of evolving pressure or current profiles and eventual MHD instability. Before AT modes can be seriously considered as an operating mode for a future fusion reactor, present experiments must sustain AT performance in a controlled manner for longer pulse lengths. In this paper, we review results of recent experiments on DIII–D directed towards this goal

The primary focus is on improving the performance and pulse length of discharges with an ELMy edge. The ELMy H–mode is inherently steady state, with the edge pressure gradient, p′, and impurity concentration regulated by the repetitive ELM events. The ELMy H–mode regime has been studied extensively on most tokamaks and the confinement results have been compiled into a database by the ITER confinement database working group. The most recent scaling for the thermal energy confinement time is given by $\tau_{th}^{98y} = 0.0365 I_p^{0.97} R^{1.93} (a/R)^{0.23} n_{19}^{0.41} B^{0.08} M^{0.2} \kappa^{0.67} P^{-0.63}$ [4]. This scaling was generated from mostly sawtoothing ELMy H–modes with monotonic q profiles and $q_0 \sim 1$.

The most serious limitation on β in long-pulse ELMy discharges appears to be the neoclassical tearing modes (NTM) [5,6]. NTM modes are classically stable tearing modes ($\Delta' < 0$) that are driven unstable by a helically perturbed bootstrap current. The NTM mode requires a seed island to exceed a minimum threshold island width; this seed island can be provided by a sawtooth crash or other MHD perturbation. The β_N limit due to NTMs in sawtoothing discharges depends on density (or collisionality ν^*), but is typically in the range $1.7 < \beta_N < 2.7$.

Our goal is to sustain higher β and confinement time relative to the ITER benchmark to achieve a more compact reactor concept with a high bootstrap fraction. The normalized quantity $\beta_N H_{98y}$ serves as a useful figure-of-merit for performance, where $H_{98y} \equiv \tau_{th} / \tau_{th}^{98y}$. The results discussed in this paper can be summarized in Fig. 1, where $\tau_{duration}$ is defined as the duration that the plotted value of $\beta_N H_{98y}$ was sustained. The squares on the left side represent typical ELM-free AT modes such as VH–mode or ELM-free NCS. They have high values of $\beta_N H_{98y}$

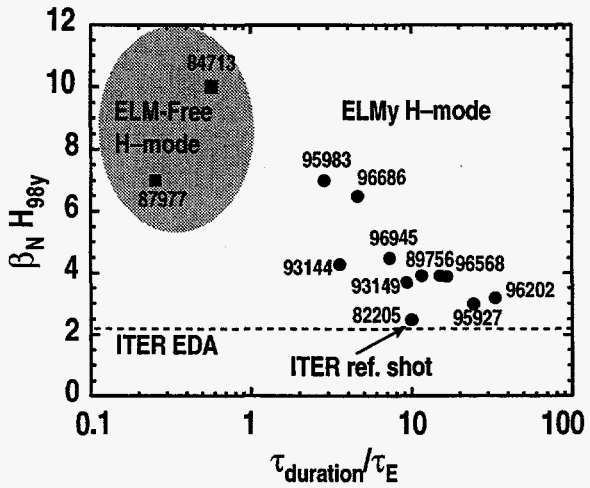

FIG. 1. Overview of performance versus duration for ELM-free AT modes (solid squares and shared region) and recent ELMy H–modes (solid circles). $\tau_{duration}$ is the duration that $\beta_n H_{98y}$ was sustained and τ_E is the energy confinement time.

but a duration of less than one energy confinement time. The circles represent best efforts from a number of different approaches to improving performance in ELMy H–mode, indicating that significant progress has been made relative to a standard "ITER-like" ELMy H–mode with $\beta_N H_{98y}$ ~2.2. While the duration varies within this group, all discharges are sustained for periods long compared with an energy confinement time. The highest performance ELMy discharges have $\beta_N H_{98y}$ ~6–8, which is comparable to typical ELM-free AT modes.

In this paper, we discuss details of several of the ELMy H–modes plotted in Fig. 1. In Section 2, nonsawtoothing discharges with monotonic q profiles (q_0~1) are presented. In Section 3, the performance of discharges with $1.5 < q_{min} < 2.5$ is described. Operating with high q_{min} is motivated by the desire to eliminate fishbones and the 3/2 surface (and possibly the 2/1 surface) so that the NTM β_N limit can be increased. This work is also motivated by the possibility of obtaining a sustained internal transport barrier (ITB) to further improve the confinement of ELMy H–modes. Finally, in Section 4 we also report on discharges obtained with a new shape and startup technique that yielded very high confinement (H_{98y} ~2) and beta (β_N~4) during a phase characterized by infrequent ELMs.

2. ELMy DISCHARGES WITH q_{min}~1

In Fig. 2, a long-pulse ELMy discharge is shown with H_{98y}~1.4 and β_N~2.8 sustained for 1.5 s. The beam power turns off just after 3.5 s in this discharge, similar discharges were sustained until 4 s. Other parameters of interest include H_{89p}~2.4, Q_{DD}~0.6×10^{-3}, and Z_{eff}~1.8. Cryopumping maintains the density at n_e/n_{Gr} ~0.3–0.5. These discharges are formed in a lower single null configuration with triangularity δ=0.3 and utilized 1.2 MW of beam power during the I_p ramp to suppress sawteeth. As seen in Fig. 2(b), the q profile is monotonic with q_0~1 and this configuration is maintained throughout the 1.5 s high power phase. Although there are no sawteeth, m/n=1/1 fishbone bursts are observed throughout the high performance phase and appear to play a role in regulating the on-axis current to maintain q_0~1. The mechanism by which fishbones regulate J(0) is not known, but we can speculate that the fishbones reconnect a small amount of poloidal flux (similar to sawteeth) or that they cause anomalously high core resistivity. The value of β_N achieved here is almost a factor of 2 above the NTM limit predicted at the operational density (collisionallity) due to the absence of a sawtooth triggered seed island (see Fig. 11). However, fishbones can also provide a seed island for the NTM and this limits both the reproducibility of this regime and attempts to further increase β_N.

The profiles shown in Fig. 1(b) and 1(c) indicate that the n_e and T_i profiles are significantly more peaked than typical ELMy H–modes, yet there is no clear ITB in the core. Rather, the improvement in confinement is is more uniform over the entire plasma radius.

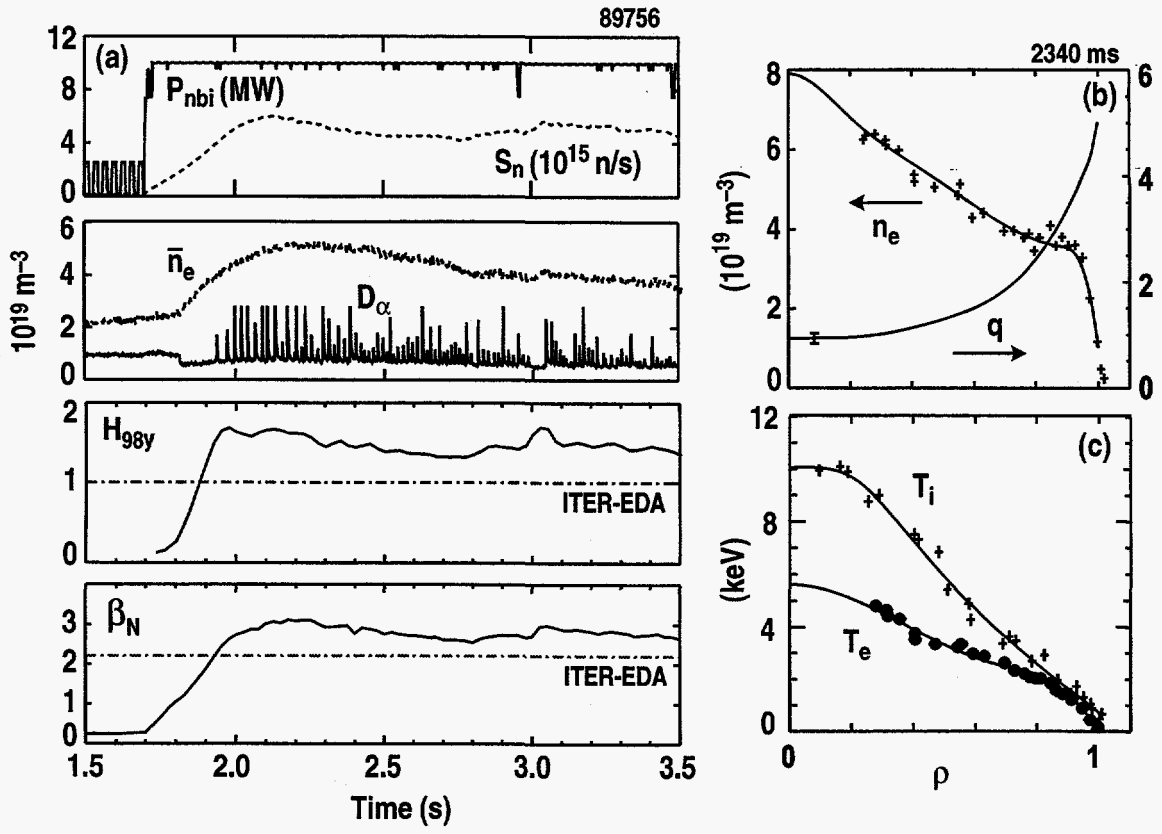

FIG.2. (a) Time evolution of ELMy H–mode 89756 (S_n = neutron rate). (b) Profiles of density and q. (c) Profiles of T_e and T_i (ρ = normalized square root of toroidal flux).

3. ELMy DISCHARGES WITH q_{min}>1.5

Current profiles with negative central shear and q_{min}>1.5 are routinely obtained by heating with P_{NBI}~5 MW during the current ramp with an L–mode edge [7]. However, the development of ITBs in these plasmas results in pressure peaking that is difficult to control and often leads to disruption. Also, because of the cold L–mode edge, the current profile and q_{min} evolve more quickly making sustainment difficult. To avoid these problems, a new startup technique has been developed using H–mode during the current ramp as shown in Fig. 3(a). A brief flat spot in the current ramp at 400 ms, coupled with the biasing of the plasma shape toward lower null point in the ion ∇B drift direction, leads to a reproducible H–mode transition. By controlling the I_p ramp rate and the density, values of ℓ_i as low as 0.5 can be obtained, although for ℓ_i <0.6 edge stability problems can lead to locked-modes during the I_p ramp. The best results are obtained with a slower I_p ramp and ℓ_i ~0.7 as shown in Fig. 3(a).

The high performance phase extends from 3.4–4 s where $\beta_N H_{98y}$~4.2 is sustained for 0.5 s. The high power phase is relatively short in this discharge due to the long formation phase and the termination of P_{NBI}. Similar discharges sustained somewhat reduced $\beta_N H_{98y}$~3.8 for 1.5 s, but

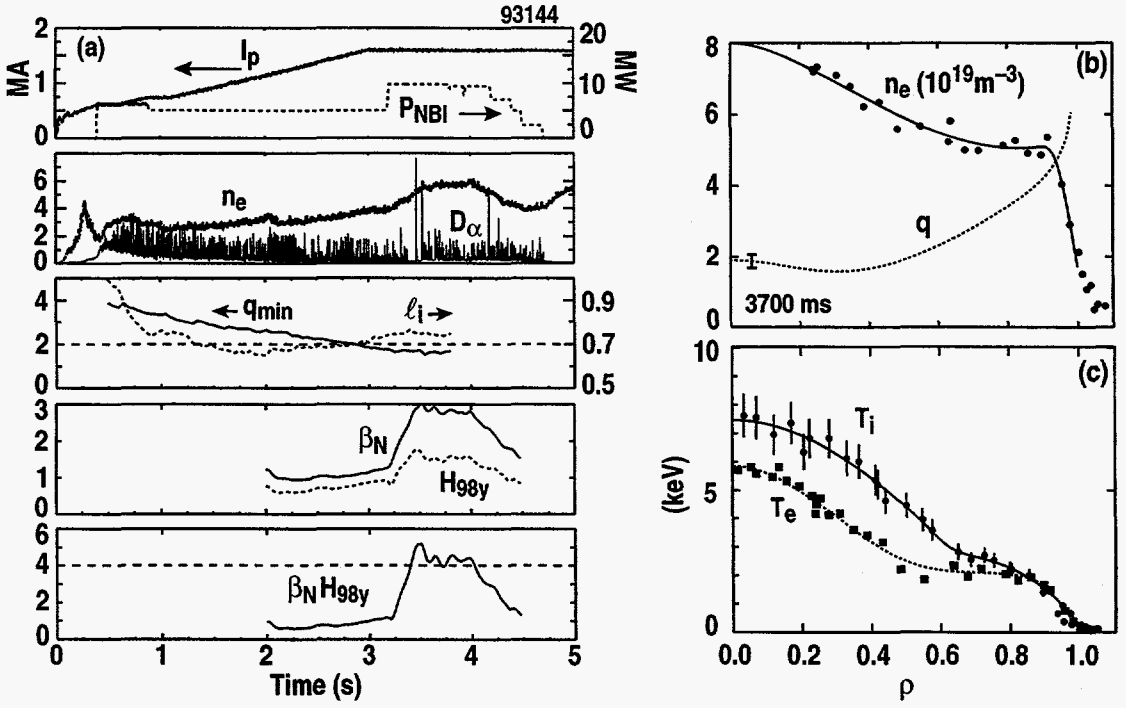

FIG. 3. (a) Time evolution of q_{min}>1.5 discharge (93144) with high performance from 3.5–4 s. (b) Profiles of n_e and q and (c) T_e and T_i at 3.7 s. (B_T=2.1 T, high triangularity shape with δ=0.77, κ=1.85; H_{89p}=2.5 at 3.7 s)

these all suffered from continuous NTM activity. Discharge 93144 in Fig. 3 is free from any significant MHD mode. The profiles of q, n_e, T_e, and T_i at 3.7 s are shown in Figs. 3(b) and 3(c). The density profile is more peaked than standard ELMy H–mode, but comparable to the other improved performance discharges such as those discussed in Section 1 with a monotonic q profile. The T_i and T_e profiles show a somewhat steeper gradient at $\rho \sim 0.5$ than is observed in monotonic q profile discharges, indicating a weak ITB. However, the ITB is much weaker here than in low density L–mode edge NCS discharges at comparable power [7]. We note that the line average density in H–mode is ~2 times that in L–mode edge NCS discharges, and with this density level we would not expect to observe strong ITBs with an L–mode edge either. The shear reversal [Fig. 3(b)] is weaker in these ELMy H–mode discharges compared with L–mode edge NCS discharges with an ITB. It could be argued that the ITB only forms with strong NCS, but there is evidence on DIII–D that ITBs can form at low density even with monotonic q profiles [8]. Rather, it appears that strong ITBs reinforce the hollow current profile through the off-axis bootstrap current, thus leading to stronger shear reversal.

Although sawteeth and fishbones are not present in the NCS discharges, NTMs continue to be the limiting instability as illustrated by the growth of a resistive m/n=5/2 mode in discharge 93149 shown in Fig. 4. This discharge is similar to 93144 in Fig. 3 except that P_{NBI} is increased to ~ 12 MW. For NTM modes, we expect the mode amplitude to scale with β_N^2, which roughly holds as shown in Fig. 4(b). The classical tearing stability parameter Δ' was calculated to be negative for this discharge indicating that it should be stable to the classical mode. Although the NTM is not catastrophic in this case, it does result in a saturation of β_N. Despite the increased

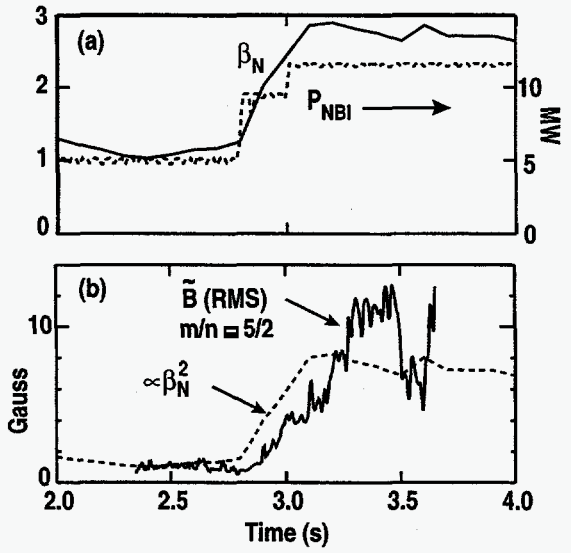

FIG. 4. (a) Time evolution of β_N and P_{NBI} for a q_{min}~2 discharge with NTM activity. (b) Fluctuation amplitude scales with β_N^2 as expected for NTMs.

P_{NBI}, β_N is actually slightly less in 93149 compared with 93144 which has no MHD mode. Note that the mode already exists at a low level in Fig. 4 prior to the step up in P_{NBI} at 2.8 s. For this series of discharges the fast magnetics data on DIII–D was set to cover the high power phase only ($t > 2.35$ s), so it is not clear what initiates the low level mode present at 2.4s. One speculation is that the mode begins as q_{min} passes through $q=5/2$ at ~ 2 s, then grows later when P_{NBI} is increased.

4. HIGH–PERFORMANCE REGIME WITH INFREQUENT ELMS

A new regime has been developed in DIII–D where performance equivalent to ELM-free modes such as VH–mode is sustained through many low frequency ELMs. As shown in Fig. 5, β_N~3.8, H_{98y}~2, and $\beta_N H_{98y}$>6 are sustained for 1 s. Lines indicating the β_N and H_{98y} values required for ITER-EDA and the ARIES-RS reactor study are also shown, indicating that this discharge exceeds the ARIES-RS requirements for the $\beta_N H_{98y}$ product. The q profile is monotonic with q_0~1 and 1/1 fishbones (but no sawteeth) are present throughout the high performance phase. Some parameters of interest during the high performance phase are: β_t~4.5%, n_e/n_{Gr}~0.5, q_{95}=4.4, τ_{th}~0.21 s and f_{bs}~50%, where n_{Gr} is the Greenwald density and f_{bs} is the bootstrap fraction. The high performance phase is terminated at ~3 s by the initiation of a m/n=2/1 NTM. Although difficult to judge from Fig. 5, when the NTM begins, the ELM frequency increases to a level more typical of ELMing H–modes at these operational parameters.

Determining the key elements for accessing this regime is still under investigation, but several operational characteristics can be identified. The initiation of a discharge similar to that shown in Fig. 5 is shown in Fig. 6. This discharge reaches slightly higher values of β_N and H_{98y} compared with Fig. 5, but the duration is shorter ~0.7 s. The discharge begins with a fast I_p ramp of ~10 MA/s to 1 MA, followed by a slow ramp rate to the final current of 1.6 MA. Beam power of 5 MW is injected at 0.1 s, leading to an extremely hollow J profile (ℓ_i ~0.3) with ρ_{qmin}~1 at 0.2 s. MHD modes due to the unstable skin current profile cause the current to penetrate rapidly leading to a weak NCS profile at 0.5 s. By the time the beams step up to full power (co-current beam injection), the q profile has evolved to be monotonic with q_0~1, ℓ_i~1.1, and fishbones are present.

An important feature of these discharges is the plasma shape (see bottom of Fig. 6). A high triangularity (δ=0.77, κ=1.85) single null shape with the X–point at the top of the vessel is utilized. The ion ∇B drift direction is down which raises the H–mode transition power threshold significantly. With this shape it takes 0.5 s at P_{NBI}=9.5 MW before the H–mode transition occurs. This long L–mode phase allows an ITB to form prior to the H–mode transition (H_{98y} ~ 1 in L–mode at 2 s) which enhances the performance after the H–mode transition is made. This technique has been used previously to maximize the fusion power in DIII–D [1], but in these earlier discharges the double null shape was symmetrized after the H–mode transition and high performance extended through the ELM-free phase only. In the discharges shown in Figs. 5 and 6, the shape remains single null with the X–point at the top and close to the wall throughout the discharge.

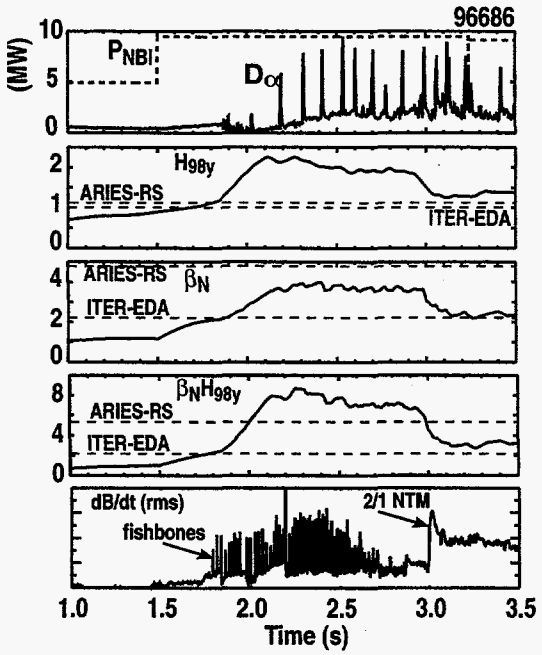

FIG. 5. Time evolution of discharge 96686 with β_N ~3.8 and H_{98y}~2 (H_{89p}~3.2) sustained for 1 s during infrequent ELMs. Dashed lines indicate the ITER-EDA design and ARIES-RS reactor study requirements for β_N and H_{98y}.

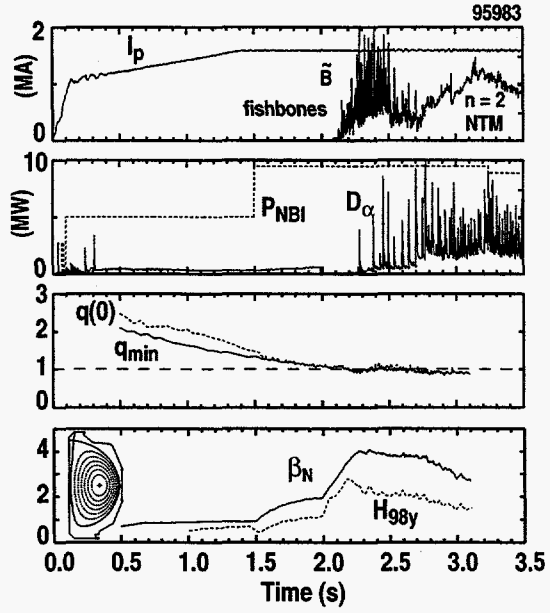

FIG. 6. Time evolution of 95983, illustrating the formation phase and q profile evolution. β_N~3.9 is sustained during infrequent ELMs from 2.2–2.7 s.

The exact importance of the startup and plasma shape is not clear. Since the target q profile is simply monotonic with q_0~1, we believe that the early fast I_p ramp and early beam power should not be critical. However, we have been unable to reproduce this regime without a startup similar to that used in Fig. 4. The shape probably plays a more important role, since edge stability is sensitively dependent on edge parameters such as p', J_{95} and collisionality. Also, the close proximity of the X–point to the wall results in higher than usual recycling near the X–point.

The infrequent ELMs also appear to play a significant role in achieving sustained high confinement. In Fig. 7, the time between ELMs (τ_{ELM}) is plotted versus the H_{98y} at the time of the ELM for several discharges. For τ_{ELM}<20 ms, confinement is close to standard ELMy H–modes with H_{98y}~1 (this represents the later part of these discharges after beta collapses). As τ_{ELM} increases to ~100 ms, confinement similar to VH–mode [9] levels is obtained. The energy loss per ELM can be quite large in this regime, ranging from 2%–5% of the plasma stored energy. With the long period between ELMs, however, the stored energy quickly recovers after the ELM. Infrequent ELMs are necessary but not sufficient to achieve the higher performance. For example, low power ELMy discharges often have infrequent ELMs but the confinement is not significantly improved.

Another factor in these discharges is that the toroidal rotation and the resulting radial electric field and E×B shear are sustained through the infrequent ELMs. For discharge 95983 in Fig. 6, $v_\phi(0)$~320 km/s and $E_r(\rho\sim0.5)$ ~120 kV/m are sustained from 2.2–2.7 s.

Profiles for discharge 95983 during the infrequent ELM phase (2.45 s) are shown in Fig. 8(a–c). Compared with other high performance modes such as VH–mode, the density profile is more peaked and the edge density gradient is reduced. Although Z_{eff} is above 2 over the entire radius due to the high power beams and fast I_p ramp early in the discharge, the edge value of Z_{eff} is actually less than other ELM-free AT modes where impurities (especially carbon) tend to accumulate at the edge. The ion and electron temperatures in Fig. 8(b) are broad with an almost linear slope from the pedestal to the magnetic axis. Thermal diffusivities calculated from TRANSP are plotted in Fig. 8(c), where an average over the time period 2.4-2.6 s has been taken to smooth the effect of ELMs. While χ_e remains anomolously high, χ_i is reduced to within a factor of 2–3 times the neoclassical prediction. Again, there is no indication of a sharp ITB, just an overall reduction in χ_i across the entire plasma. During the transient ELM-free phase earlier in the discharge, χ_i is estimated to be approximately equal to the neoclassical value as seen previously in other high performance discharges [1].

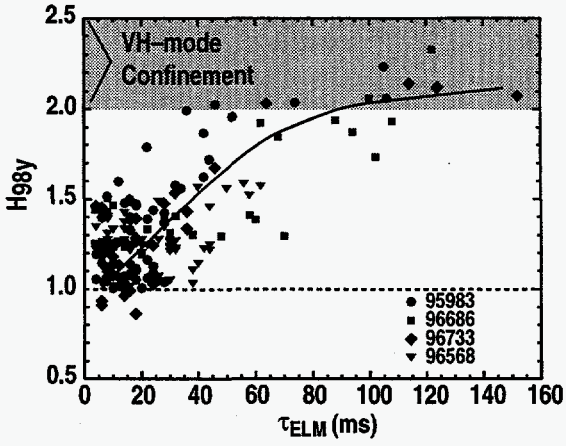

FIG. 7. Confinement enhancement, H_{98y}, improves with period between ELMs. Shaded region indicates typical confinement range for VH–modes on DIII–D.

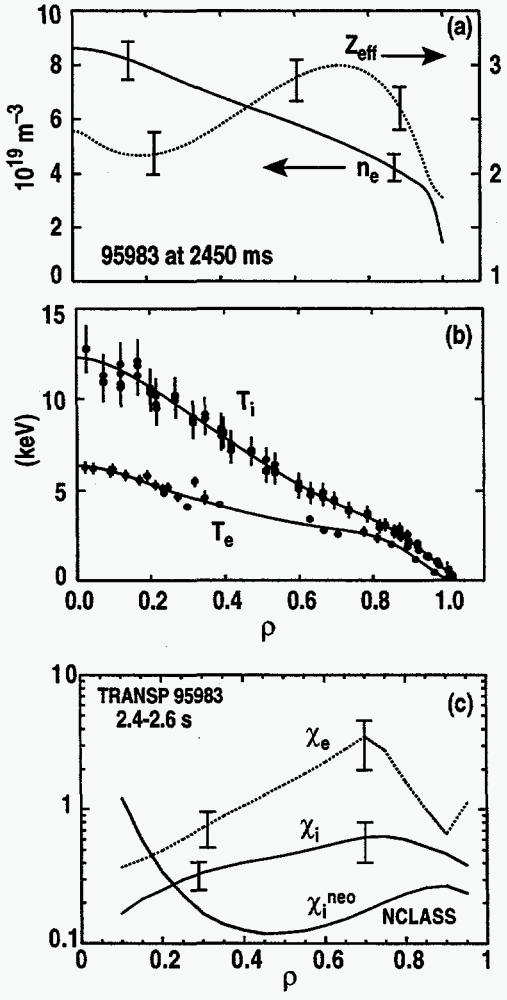

FIG. 8. (a–e) Profiles for 95983 at 2.25 s, just before the first ELM (solid curves and plus symbols) and VH–mode profiles (83710 at 2.75 s) just before the first ELM (dashed curves and sold circles). (f) χ profiles for 95983 during ELMs (2.4-2.6 s) calculated from TRANSP.

4.1. Edge Stability Analysis

The discharges shown in Figs. 5 and 6 do not collapse at the first ELM as do VH–modes [10], for example. Early speculation on why these ELMs are more benign focused on the possibility that the edge p' was reduced. Although the density gradient is substantially reduced compared with typical VH–modes, the temperatures are higher, so that the final edge pressure gradient and pedestal height are actually higher in 95983 than VH–mode. Profiles of q, p, and $\langle J_{||} \rangle$ from a kinetic efit prior to the first ELM at 2.25 s are shown in Fig. 9. The EFIT equilibrium reconstruction utilizes external magnetic measurements, MSE data–including E_r corrections–and pressure profiles including the calculated fast ion contribution. The q profile shows a large flat region with q~1 while the current density shows a large edge current peak due to the edge p' and the resulting bootstrap current. Calculation of the bootstrap current density is shown in Fig. 9(c) where the location and amplitude of the bootstrap peak is in good agreement with measurements. Note that the overall current at the edge is somewhat reduced because the edge surface voltage is actually negative during the ELM-free phase leading up to this time. Ballooning and Mercier stability have been calculated with the results plotted in Fig. 9(d). The reduction in edge shear due to the edge bootstrap current opens up 2nd stability access at $\rho \sim 0.95$ which allows the high edge pressure gradient. This result is typical of most ELM-free high triangularity plasmas on DIII–D. The core is Mercier unstable due to low value of q inside $\rho \sim 0.35$ and the large pressure gradient in this region. We note that recent theoretical work on the stabilizing effects of fast ions [11] and/or rotational shear may modify the Mercier criterion in this region.

GATO calculations of ideal n=1–4 stability has also been performed for this timeslice. In general, GATO predicts that this regime is marginally stable to n=1–4 edge "peeling" modes, although depending on the exact details of how the input equilbria is prepared, GATO can also find these modes to be unstable. Stability of edge modes with $n \geq 5$ cannot be calculated with GATO. Thus, it is not clear if the large infrequent ELMs observed are due to the peeling mode or not. The important point, however, is that experimentally there seems to be no coupling between the edge mode and a more destructive global mode. The reasons for this are not known, but we suspect that unique features of the shape and edge current profile may be playing a role. Despite the large current spike observed at $\rho \sim 0.95$ in Fig. 9(c), the average current from $0.75 < \rho < 1$ is not so high at this time because the surface loop voltage is slightly negative. Also, the current density at $\rho \sim 1$ is lower than usual because of the reduced ∇n_e at this location. Both of these effects are favorable for stability.

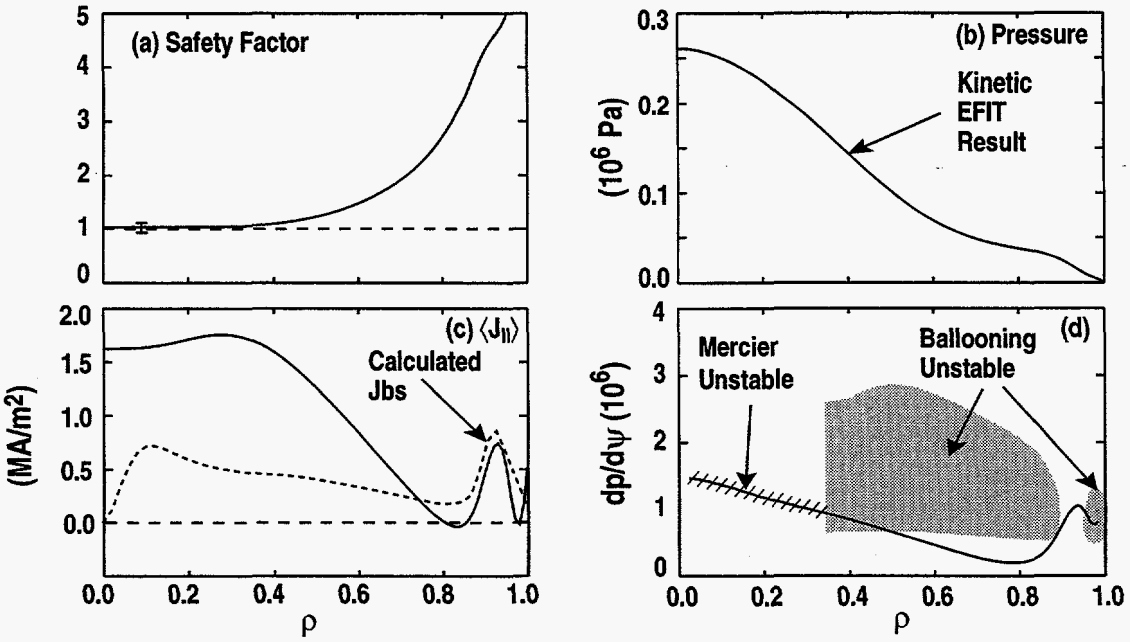

FIG. 9. (a–c) Kinetic EFIT equilibrium profiles for 95983 at 2.25 s. The dashed line in (c) represents the calculated bootstrap current density for the profiles shown in Fig. 6. (d) Ballooning/Mercier stability diagram at 2.25 s. The solid curve is the experimental value of dp/dψ.

4.2. Neoclassical Tearing Modes

All of the discharges produced to date that achieve high performance (β_N>3.5) during ELMs revert to a standard H–mode with a soft beta collapse accompanied by MHD activity that has the characteristic signature of the NTM. These characteristics are that (1) $\Delta' < 0$ indicating modes are classically stable; (2) a seed island threshold width must be exceeded before the mode can grow; (3) the mode amplitude saturates at a level that can be predicted by NTM theory and is $\propto \beta_N^2$. Since none of these discharges have sawteeth, the seed island must be generated by another mechanism. In many cases fishbone bursts provide the seed island, although there are also cases where the NTM trigger is not so clear. For discharge 95983 in Fig. 6, the NTM clearly starts to grow after a fishbone burst as shown in Fig. 10. Here contours of constant mode amplitude are plotted for n=1 (dark shade) and n=2 (light shade) modes. In addition to the 1/1 fishbone bursts and the associated second harmonic, one can observe the coupled 3/2 mode at ~38 kHz. The first few 3/2 bursts die away, but at 2.73 s the 3/2 mode becomes continuous and begins to grow. The 3/2 mode number has been confirmed by analyzing the poloidal magnetic probe array and by comparing the 3/2 mode frequency with the fluid rotation velocity at the q=3/2 surface. Both the seed island width and the saturation amplitude have been estimated from Mirnov signals for this discharge and agree with predictions from NTM theory.

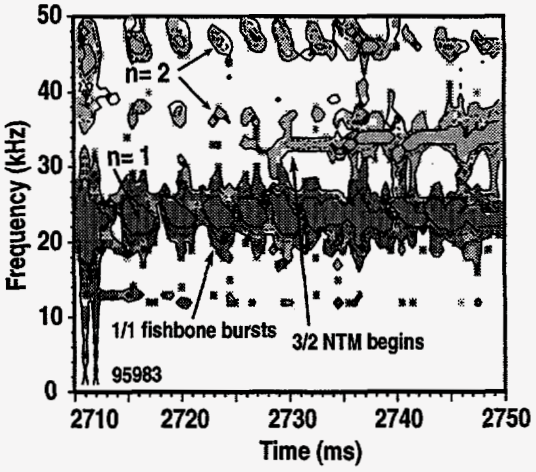

FIG. 10. Contours of constant B-dot mode amplitude for n=1 (dark shade) and n=2 (light shade) modes. A continuous 3/2 mode is triggered by a fishbone burst at 2730 ms.

While NTM modes appear to limit β_N in many of the high performance ELMy H–mode discharges discussed in this paper, the β_N limit is significantly higher than the limit observed in sawtoothing ITER-like discharges. In Fig. 11, the critical β_N for onset of NTMs is plotted versus a function of density (or collisionality ν^*) as determined by La Haye, *et al.* for sawtoothing ITER-like discharges [12]. The β_N limit for the high performance ELMing H–mode discharges discussed in this paper are also plotted and range from 50% to 100% higher than the sawtoothing limit. Despite this success in raising the NTM β limit, the NTM modes limit our ability to further increase β and, since the time at which the seed island triggers the mode varies considerably from shot to shot, the reproducibility of these discharges is poor. Techniques to calculate and produce profiles that are more robustly stable to these modes is an important next step.

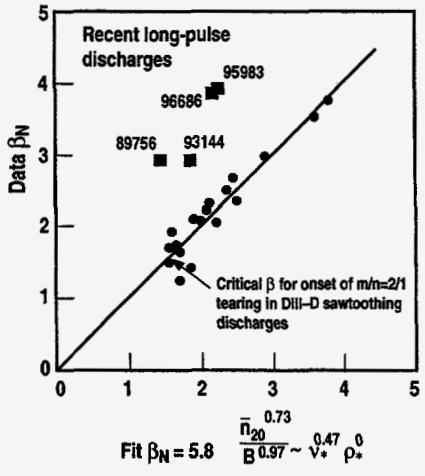

FIG. 11. The beta limit for discharges discussed in this paper (squares) exceed the NTM limit established for sawtoothing discharges (circles and line) by a factor of ~2.

5. DISCUSSION

Improved performance has been achieved in a variety of ELMy H–mode discharges in DIII–D. With normal-frequency ELMs (50–100 Hz), H_{98y}~1.4 (H_{89p}~2.5) and β_N~2.9 has been sustained for ~ 1.5–2 s (10–15 τ_E) in discharges with both monotonic (q_0~1) and NCS q profiles. The absence of sawteeth in these discharges plays an important role in accessing higher confinement and β relative to the ITER benchmark. In the NCS discharges, sawteeth are simply eliminated by raising q_{min} well above unity. In the monotonic q profile discharges, fishbones appear to play a role in maintaining q_0 at, or slightly above, unity, thus preventing sawteeth.

By removing the core sawtooth instability, more-peaked density and temperature profiles and larger core rotation (E×B shear) are observed, enabling a ~40% increase in global confinement compared with the ITER98y scaling. Although core confinement is improved in these discharges, the sharp localized ITBs seen in L–mode edge NCS discharges are not observed here.

Regarding stability, the absence of sawtooth induced seed islands allows β_N values up to 2 times the previously established sawtoothing neoclassical tearing mode limit. In spite of this, NTMs triggered by other MHD events (fishbones, ELMs) remain a limitation to both the reproducibility of long-pulse discharges and further attempts to increase β_N.

A new regime characterized by infrequent ELMs ($\leq$ 10 Hz) has produced performance comparable to VH–mode, but sustained for longer pulse lengths. The best of these discharges produced H_{98y}~2 (H_{89p}~3.2) and β_N~3.8 for 1 s (~5τ_E). Again, here the q profile is monotonic with q_0~1 and there are fishbones but no sawteeth. Ion thermal diffusivity is reduced over most of the discharge to ~2–3 times neoclassical. Although the ELMs are not small in this regime (2%–5% energy loss per ELM), they are benign in the sense that no global MHD mode is triggered that could cause a core β collapse. The long period between ELMs allows the stored energy and toroidal rotation time to recover, giving confinement properties that are closer to ELM-free regimes than usual ELMy regimes. The pulse length of most of these discharges is ultimately limited by the triggering of resistive NTMs rather than ideal MHD modes that terminate typical VH–modes.

The explanation for improved performance in these discharges is still under investigation, but we can identify several features that may be important. First, the upper single null high-triangularity shape has a high H–mode power threshold that results in a long enhanced L–mode phase. Upon the H–mode transition, high performance is obtained rapidly, before the current density in the edge region can fully develop. Although a large bootstrap peak at ρ~0.95 is observed, the average current density in the region $0.8 < \rho < 1.0$ is not so large and this is

beneficial for stability to edge peeling modes. Also, the X–point is located close to the wall in these discharges which results in larger recycling near the X–point. This may have a subtle effect on details of the edge profiles and gradients. In comparison with a typical VH–mode, although the edge pressure gradient is comparable, the infrequent ELM discharges have reduced edge density gradients. Finally, we note that the q profile, although monotonic, has a somewhat broader shape (larger volume with q~1) than previous discharges.

Future plans include making use of the upcoming high-power electron cyclotron current drive (ECCD) system on DIII–D. By driving current off-axis, we will be able to achieve improved control over the q profile and can sustain the q profile for longer pulse lengths. The ECCD system will also be used for experiments on stabilizing NTMs, which are a significant limitation in long-pulse discharges.

REFERENCES

[1] LAZARUS, E.A., *et al.*, Phys. Rev. Lett. **77** (1996) 2714.

[2] KOIDE, Y., *et al.*, Phys. Plasma **4** (1997) 1623.

[3] SOLDNER, F.X., *et al.*, Plasma Phys. Control. Fusion **39** (1997) B353.

[4] ITER Physics Basis Document, to be published in Nuclear Fusion. JET report JET-P(98)17.

[5] CHANG, Z., *et al.*, Phys. Rev. Lett. **74** (1995) 4663.

[6] LA HAYE, R.J. and SAUTER, O., Nucl. Fusion **38** (1998) 987.

[7] RICE, B.W., *etal.*, Nucl. Fusion **36** (1996) 1271.

[8] RICE, B.W., *et al.*, in Controlled Fusion and Plasma Physics (Proc. 25th EPS Conf. Prague, 1998) Vol. 22C European Physical Society, Geneva, (1998) 826.

[9] JACKSON, G.L., *et al.*, Phys. Rev. Lett. **67** (1991) 3098.

[10] FERRON, J.R., *et al.*, in Controlled Fusion and Plasma Physics (Proc. 21st EPS Conf. Montpellier, 1994) Vol 18B, Part I, European Physical Society, Geneva, (1994) 86.

[11] PORCELLI, F. AND ROSENBLUTH, M.N., Plasma Phys. and Contr. Fusion **40** (1994) 481.

[12] LA HAYE, R.J., *et al.*, in Plasma Physics and Controlled Nuclear Fusion Research 1996 (Proc. 16th Int. Conf. Montreal, 1996), Vol. 1, IAEA, Vienna (1997) 747.

ACKNOWLEDGMENT

Work supported by U.S. Department of Energy under Contracts DE-AC03-89ER51114, DE-AC02-76CH03073, DE-AC05-96OR22464, and W-7405-ENG-48.